

Molecular dynamics simulation of synchronization in driven particles

Tiare Guerrero* and Danielle McDermott†

Department of Physics, Pacific University, Forest Grove, OR 97116

(Dated: December 23, 2020)

We discuss a numerical model of particles confined to a narrow channel driven across a washboard potential energy landscape. The model exhibits synchronization effects that provide insight to the behavior of experimental systems including magnetically driven colloidal particles confined by light-fields. We present the basics of the molecular dynamics simulations for particles moving through a viscous liquid applied to single and multiple particle systems. We demonstrate how to visualize the system with animations of the particle motion and detect synchronization using measurements of the particle velocity as a function of applied driving force. We include sample code and exercises for students with opportunities to reproduce our results and propose new numerical experiments. With only a few particles in two-dimensions, the simulation runs quickly, making this an appropriate model for undergraduates to explore.

I. INTRODUCTION

Synchronization is a universal phenomena in which individual oscillators adjust frequency due to interaction or an external stimulus [1]. Synchronous behaviors where oscillators move in-phase (i.e. in time) are observed in many everyday systems such as the flickering candle flames coupled by temperature fluctuations [3] and metronomes coupled through the the supporting table [4]. Biological systems benefit from cooperative synchronization such as when birds coordinate flapping of wings in order to optimize energy use during flight [5], frogs communicate by croaking patterns modulated by location [6], and humans synchronize clapping in time with music [7]. At a cellular level, neurons simultaneously fire in cardiac muscle [8] and brain tissue [9].

A particular form of synchronization is phase-locking, which first appeared in the scientific literature with Huygens' 1665 experiments on the motions of two pendula on wall-mounted clocks. Huygens demonstrated the tendency of two periodic oscillators in close proximity to swing in time due to interactions through the wall no matter the original phase of the clocks [2]. Dynamical systems exhibit phase-locking when oscillators with different frequencies couple so the frequency ratio or mode is an integer number [11]. This can be demonstrated with Lissajous figures, i.e. parametric graphs of two periodic functions which make looped patterns determined by the mode, first reported in 1857 [12] and easily generated with a computer code or oscilloscope [13].

Synchronization is often achieved via external forcing such as when pushing a child on a swing at the high point on her path, or using pacemaker (an electrical generator) pulses to regulate a heart beat. [Fireflies and pulsed LED].

Dynamical mode locking has many important technological applications and is often studied with simplified

computational models. These studies can be performed with coupled oscillators [?] or with a single particle driven across a periodic potential landscape [].

Synchronization is observed in quantum electronic devices such as Josephson junctions [14, 15] i.e. two superconductors sandwiching an insulating layer. When subject to an external voltage, Cooper pairs in the superconducting materials tunnel through the insulating layer. Phase-locking is observed as stepped regions in current-voltage (I-V) relationship in these devices, where a constant current results from a range of voltages due to the quantized nature of the tunneling probability [NOT QUITE RIGHT...]. Known as Shapiro steps [17], these indicators of phase locking have been observed broadly in a variety of systems either in velocity-force curves and voltage-current curves [18]. Shapiro steps are hallmarks of non-Ohmic behavior in voltage-current curves, where these steps are generated by the tendency of the response of a system to be flat across a range of applied driving forces or voltages, which can be probed with applied AC forces.

Recent experiments of particles confined in optical traps subject to external driving forces have been used to examine the microscopic dynamics of mode-locking in colloids interacting via magnetic dipole or electrostatic interactions in experiment [20, 23] and simulation [21, 22]. Colloidal particles trapped in light fields are a particularly useful medium for studying complex dynamical behaviors. Colloid particles are micron-sized, a relatively large size to control and image. The interaction forces between colloids can be modified by tuning the chemistry of the suspending fluid or surface ligands of the colloidal particles [?]. This ease in control of colloids has lead to a rich array of experimental results considered models for experimental systems relatively hard to access and visualize, such as cold atoms or electron gases.

Particles which interact over long distances include colloids, magnetic beads, superconducting vortices, dusty plasmas, electron gases. [more detail and references] Particles which interact over short distances include bubble arrays/emulsions [more systems and references].

Particles in confined geometries behave differently than

*Electronic address: guer9330@pacificu.edu

†Electronic address: mcdermott@pacificu.edu

free particles. Stabilized charged particles form patterns due to the interplay of the confining environment and particle interactions. Narrow channels studies are useful to provide insights of how particles move through systems such as wires and microchannels. Biological systems such as neuron axons and capillaries can also be studied with these models [more detail and references]. Many such systems execute local oscillations about stable points [elaborate]. The presence of a modulating surface can modify these patterns in a variety of ways, changing the onset of dynamical flows, and the overall flow patterns.

The dynamics of particles subject to an applied external force apply to many physical systems. For instance the flow of charges in a conductor, or cells responding to a chemical gradient. The external force increases the diversity of dynamical behaviors, and can cause particles to flow in a variety of non-linear complex patterns that may be synchronized. Disordered chaotic dynamics are also possible, where irregular, unpredictable time evolution of nonlinear systems occurs in mechanical oscillators [?].

Numerical modeling of colloids can provide mechanistic insight that can be difficult to achieve in experimental conditions where Brownian motion and other sources of noise dominate. [elaborate]

Here we focus numerical studies of the synchronized dynamics of confined particles driven over a washboard shaped potential energy landscape. We chose this model for its relevance to condensed matter systems and ease of simulation. The period of the substrate can be used to control the intrinsic velocity of the driven particle.

In this work, we perform numerical simulations of confined, driven particles to model a variety of physical phenomena. In the following paper we describe our molecular dynamics model in Section II. We include code to simulate and visualize the dynamics in this section and supplementary material. In Section III we summarize our results, including synchronized motion of a single confined particle driven across a periodic landscape in Section III A and multiple interacting particles in Section III B, including stationary propagation of high density kinks in Sec. III C. We present these results using standard tools of non-linear oscillators such phase diagrams of velocity versus position. In Section IV, we show how an aperiodic landscape modifies the particle dynamics. Finally we explore the transition to chaotic dynamics in Section V and conclude in Section VII. In each section we suggest exercises for interested students, as summarized in Section VI.

II. MOLECULAR DYNAMICS MODEL

We use a classical two-dimensional model for studying the dynamics of N interacting particles. Particles are confined in a two-dimensional (2D) simulation of area $A = L \times L$ where $L = 36.5a_0$ where a_0 is a dimension-

less unit of length. An individual particle i has position $\vec{r}_i = x_i\hat{x} + y_i\hat{y}$. Particles are subject to periodic boundary conditions such that a particle leaving the edges of the system is mapped back to a position within the simulation by $x_i + L = x_i$ and $y_i + L = y_i$. The units of the simulated variables are in Table I.

TABLE I: Simulation units.

Quantity	Unit
length	a_0
energy	$E_0 = q^2 Z^{*2} / 4\pi\epsilon\epsilon_0 a_0$
dimensionless interaction strength	q
effective colloidal charge	Z^*
solvent dielectric constant	$\epsilon\epsilon_0$
force	E_0/a_0
viscosity/damping constant	η
time	η/E_0
velocity	$E_0/\eta a_0$

We model particle interaction forces $\vec{F}_{ij} = -\nabla U_{ij}(r_{ij})$ with the Yukawa potential energy

$$U_{ij}(r_{ij}) = \frac{E_0}{r_{ij}} e^{-\kappa r_{ij}}, \quad (1)$$

where particle i and j are distance $r_{ij} = |\vec{r}_i - \vec{r}_j|$ apart. This screened Coulomb potential is scaled in terms of energy unit E_0 defined in Table I. $\kappa = 1/R_0$ is the screening parameter that describes the lengthscale at which particles interact. We fix R_0 to be a_0 . In experiments charge screening is observed due to ions in the suspending fluid and the charges of surrounding particles which reduces the interaction range of individual particles. Because the particles interact over short ranges, the numerical models can be run efficiently using a neighbor list algorithm determined using a cell method. [explain!]

Particles are subject an external time-dependent driving force $\vec{F}_D(t)$ applied parallel to the y -direction. We model this force as

$$\vec{F}_D(t) = [F_{DC} + F_{AC} \sin(\omega t)]\hat{y}, \quad (2)$$

with modifiable parameters including a constant component F_{DC} , and a time dependent component with amplitude F_{AC} and frequency $\omega = 2\pi f$.

We use several model environments to confine the particles, assuming the confining force arises from a potential function $\vec{F}_i(\vec{r}) = -\nabla V_i(\vec{r})$. The landscape potential $V(\vec{r})$ are static with fixed minima and maxima that are periodic or quasi-periodic, as described in Sec. III. In multi-particle simulations, we confine the particles along the x -direction using a periodic function

$$U_{q1D}(x) = U_0 \cos(\pi x/L) \quad (3)$$

. This quasi-one-dimensional geometry confines the particles primarily to move along the y -direction but allows

for some lateral motion of particles. Otherwise the repulsive interaction between particles would cause them to spread throughout the system.

The simulation is controlled by a *for()* loop which runs from an initial to maximum *time* integer. Each integer timestep represents a simulation time of $\Delta t = 0.001$. At each timestep we evaluate the net force on each particle as a function of its position $\vec{r}_i(t)$ and then integrate the equation of motion to move particles to an updated position $\vec{r}_i(t + \Delta t)$. The integration is simple because we model the particle dynamics with an overdamped equation of motion. The damping comes from a viscous fluid model providing a nonconservative force, modeled as a linear friction $\vec{F}_{drag} = -\eta \vec{v}_i$ sufficient so that the acceleration of the particle is zero. Such a model is appropriate when the particles are small and the viscosity is high [finish... reference...] This model should be familiar to readers modeling Milliken's oil drops in a standard classical mechanics text [?].

A particle has the equation of motion

$$\eta \vec{v}_i = \vec{F}_{l,i} + \sum_{i \neq j}^N \vec{F}_{ij} + \vec{F}_D(t). \quad (4)$$

where $\eta = 1$. The equation of motion provides a direct calculation of the velocity of an individual particle from its location in the simulation with respect to other particles j . Since the acceleration is zero, the Verlet method simplifies to the Euler method, which is used to calculate the position at subsequent time steps.

$$\vec{r}_i(t + \Delta t) = \vec{v}_i(t) \Delta t + \vec{r}_i(t). \quad (5)$$

III. RESULTS

We demonstrate how a single particle (Sec. III A) and many particles move (Sec. III B) in response to this applied force in a variety of environments. In Sec. III C we set F_{DC} to zero and track the motion of a high density area of a particle chain (i.e. kink dynamics).

A. Single particle system

We drive a single particle across a periodic landscape along the y -direction

$$V_l(y) = V_{0y} \cos(N_p \pi y / L) \quad (6)$$

with $N_p = 20$ troughs in the landscape. This is illustrated in Fig. 2(a) where the red (blue) regions show local maxima (minima). The code for generating a two dimensional colored plot of the potential landscape is calculated by evaluating the analytic function in Eq. 7 for a grid of values (x_n, y_n) . The numerical implementation of the landscape is calculated with

$$F_y(y) = F_{0y} \sin(N_p \pi y / L) \quad (7)$$

where $F_{0y} = 0.1$. We drive the particle with $F_{AC} = 0.2$, $F_{DC} = 0.01$, and $f = 0.01$ cycles per time unit. When the superposition of F_{AC} and F_{DC} is large enough to overcome the barrier height of the landscape troughs, the particle hops between troughs in the energy landscape. In Fig. 1 we show the relationship between the applied force and particle position. In Fig. 1(a) we plot the applied driving force as a function of time and in Fig. 1(b) we show the position of the particle as a function of time. The initial position is near $y = 0$ and the initial driving force is minimum $F_D(t = 0) = F_{DC}$. Over the time period $T/2 = 50$ the particle moves in the positive y -direction while $F_D(t) > 0$ through three substrate troughs, reaching a maximum of $y/\lambda = 3$. When $F_D(t) < 0$ the particle moves in the negative y -direction reaching a minimum position of $y/\lambda = 1$ over the period $T = 1/f = 100$. The average velocity \bar{v}_y is the average displacement $\Delta y = y(t_0 + T) - y(t_0)$ over the period of the driving force. In Fig. 1 the displacement is a single wavelength of the substrate $y(t_0 + T) - y(t_0) = \lambda$. Thus the average velocity is $\bar{v}_y = \lambda f$, where $T = 1/f$.

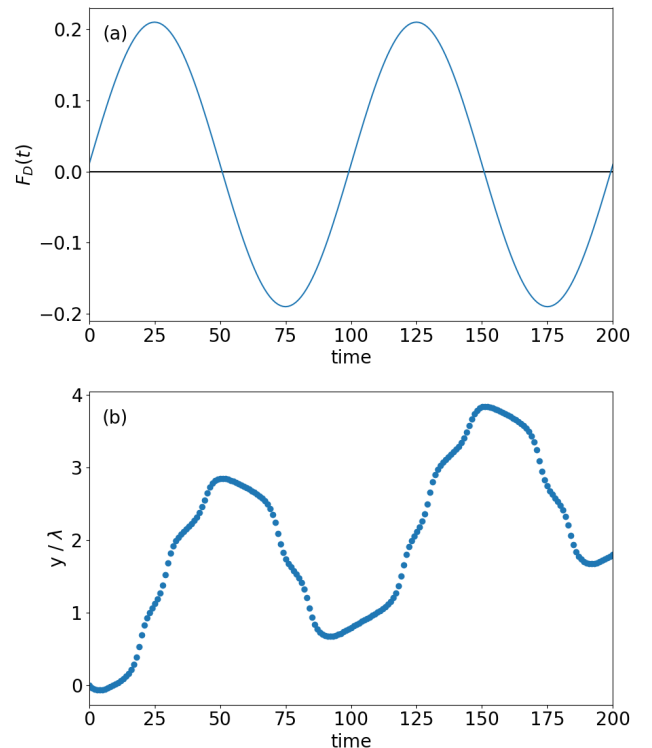


FIG. 1: The position as a function of time of a single driven particle normalized by the period of the substrate λ .

The hopping pattern of the driven particle is periodic, and could be achieved over a range of F_{DC} . We explore the ranges of periodic hopping patterns by increasing F_{DC} as a function of time, as shown in Fig. 2. We apply an external applied force, with a constant F_{AC} with

frequency $\omega = 2\pi f$ then slowly increase F_{DC} at a rate of $\Delta F_{DC} = 0.001$ every $\Delta t = 4000$ integer timesteps or 40 time units. By modifying F_{DC} we achieve a variety of oscillation modes. A mode is a periodic pattern of hops with a constant average particle velocity, \bar{v}_y over a range of driving forces F_{DC} . We illustrate mode-locking in the velocity-force plot in Fig. 2(b). Here \bar{v}_y is increasing in non-uniform steps, with a quantized height of $\bar{v}_y = n\lambda f$, where n is an integer, $\lambda = S_Y/N_p = 36.5/20 = 1.825$ is the spatial period, or wavelength of the landscape, and $f = 0.01$ cycles per time unit.

Our simulations reproduce results presented in Juniper *et al.* [20] which demonstrated mode locking in experiments of driven colloids on a optical periodic landscape.

We illustrate the hopping pattern in Fig. 2(b) and show the dynamics in supplementary materials [24].

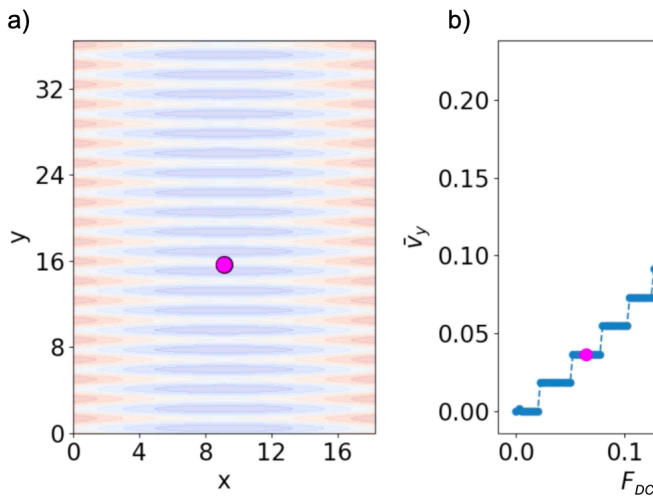


FIG. 2: (a) The particle is driven with a constant amplitude F_{AC} and frequency ω through a periodic spatial potential landscape. The landscape is represented with a colormap where blue are minima and red are maxima in the potential. (b) An average particle velocity in the y-direction \bar{v}_y as a function of a constant driving force F_{DC} . In the animation available in Ref. [24] the magenta dot represents the average velocity of the particle \bar{v}_y at which the particle in Fig. 1(a) is moving.

B. Synchronization in multi-particle systems

We simulated a twenty particle system confined to a narrow channel, as shown in Fig. 2a). We create the confining channel with a sinusoidal function with a single period.

$$V_l(x) = V_{0x} \cos(\pi x/L) \quad (8)$$

where the trough heights is larger V_{0x} , and the associated force

$$\vec{F} = -\nabla V(x) = -\frac{dV}{dx}\hat{x} = -\frac{V_{0x}\pi}{L} \sin(\pi x/L)\hat{x} \quad (9)$$

restores particles to the center of a long narrow region of the simulation. The landscape is illustrated in Fig. 3(a) where red regions are high potential and blue regions are low potential.

The initial configuration of the system is shown in Fig. 3(a). We annealed the system into a ground-state configuration by raising the system to a high temperature T , and slowly lowering the temperature in steps of $dT = -0.01$ until the particles form a buckled chain in the low region of the channel due to the competition between particle repulsion and channel confinement. The interparticle forces between neighboring particles cause the system to form a buckled chain. The molecular dynamics of simulated annealing is described in Ref. ??, and presented simulations begin with particle configurations that result from the annealing process, as listed in Appendix [ref] and available in supplementary material.

When a single particle is driven, the neighboring particles act similarly to a periodic landscape to impede its motion. A driven particle can exhibit mode locking with a well-chosen AC drive and frequency. In the attached movie, Figure2.mp4, we show the complex dynamics of mode locking, where the driven particle leap-frogs past the other particles.

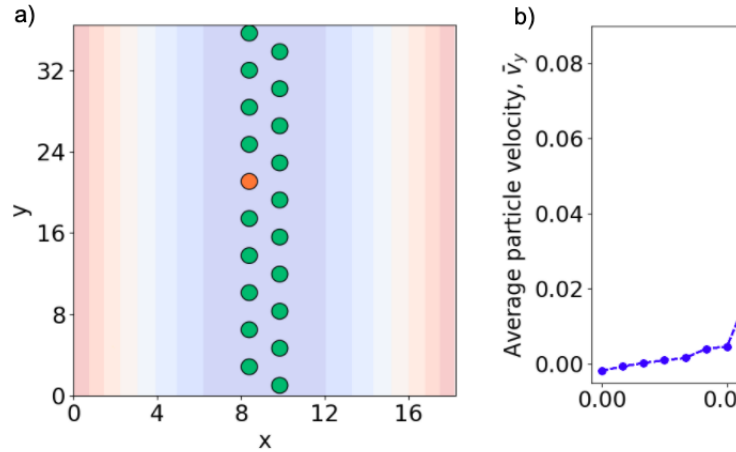


FIG. 3: (a) A single particle (colored orange - mark in some manner for non-color views) is driven with a constant amplitude F_{AC} and frequency ω through 19 neighboring particles (colored green - mark differently) confined by a quasi one-dimensional channel. The landscape is colored as in Fig. ??(a). (b) Average \bar{v}_y versus F_{DC} , where \bar{v}_y is the average particle velocity of the driven particle in the y-direction.

C. Kinked system

We confine N particles to $N - 1$ troughs to create a local high density region. $F_{DC}/F_{AC} = 1$ [CHECK!]

IV. QUASIPERIODIC SUBSTRATE

V. CHAOTIC DYNAMICS

VI. ASSOCIATED PROBLEMS

1. Kuramoto model = overdamped interacting rotors/oscillators are used to model coupled oscillator systems - no substrate or external drive so far as I can see - this seems baked into the oscillator properties/interactions
2. Brownian motion without fluid dynamics using Ermak's algorithm
3. Frenkel-Kontorova and competing length scales for low temperature systems where thermal fluctuations are negligible
4. The Fokker-Planck Equation

VII. CONCLUSION

VIII. SUPPLEMENTARY MATERIALS

A. Gridded Contour Plot of landscape

#####

#ADD CONTOUR PLOT

#####

def add_contour(ax,L,N,corrugated = True):

'''

Hardwired to color in the quasi1D potential to contain the particles in a trough.

Can also add the washboard/corrugated substrates

Required Arguments

Optional Arguments:

corrugated (default = True)

Adds the washboard in the y-direction.

Hardwired for a single parameter set.

'''

a_p = L/N

#assuming Tiare's trough system, so we won't want

X = np.arange(0, L/2.0, 0.1)

Y = np.arange(0, L, 0.1)

X, Y = np.meshgrid(X, Y)

Z_mag = 2.0 # set by what "looks good"

Z = Z_mag*np.sin(2*np.pi*X/L)

if corrugated == True:

 Z += np.sin(2*np.pi*(Y+1.75)/a_p)

cmap=cm.coolwarm_r

#alphs is the degree of transparency, again, set

cset = ax.contourf(X, Y, Z, cmap=cmap,alpha=0.25)

#ax1.set_xlim(15,20)

#ax1.set_ylim(15,20)

#ax1.set_xlabel(r"\$X\$")

#ax1.set_ylabel(r"\$Y\$",rotation='horizontal',ha='')

#ax1.set_xticks([])

#ax1.set_yticks([])

return

Acknowledgments

We acknowledge Harvey Gould and Jan Tobochnik, who invited us to write the article and supported its development. Charles and Cynthia Reichhardt advised the project and provided the original molecular dynamics code written in the C programming language. We acknowledge funding from the M.J. Murdock Charitable Trust and the Pacific Research Institute for Science and Mathematics (PRISM).

-
- [1] A. Pikovsky, M. Rosenblum, and J. Kurths, *Synchronization: A Universal Concept in Nonlinear Sciences* (Cambridge Univ. Press, Cambridge, 2003).
 - [2] M. Bennett, M.F. Schatz, H. Rockwood, and K. Wiesenfeld, Huygen's clocks, Proc. Roy. Soc. A **458**, 563 (2002).
 - [3] K. Okamoto, A. Kijima, Y. Umeno, and H. Shima. Synchronization in flickering of three-coupled candle flames. Sci Rep **6**, 36145 (2016)
 - [4] J. Jia, Z. Song, W. Liu, J. Kurths, and Xiao, J. Experimental study of the triplet synchronization of coupled

nonidentical mechanical metronomes. Sci. Rep. **5**, 17008 (2015).

- [5] S. Portugal, T. Hubel, J. Fritz, S. Heese, D. Trobe, B. Voelkl, S. Hailes, A. M. Wilson and J. R. Usherwood. Upwash exploitation and downwash avoidance by flap phasing in ibis formation flight. Nature **505**, 399 (2014).
- [6] I. Aihara, T. Mizumoto, T. Otsuka, H. Awano, K. Nagira, H. G. Okuno and K. Aihara. Spatio-Temporal Dynamics in Collective Frog Choruses Examined by Mathematical Modeling and Field Observations. Sci Rep **4**, 3891 (2014).

- [7] P. Tranchant, D. T. Vuvan, and I. Peretz, Keeping the Beat: A Large Sample Study of Bouncing and Clapping to Music. PLoS ONE 11(7): e0160178. (2016).
- [8] G. Martin Hall, Sonya Bahar, and Daniel J. Gauthier, Prevalence of Rate-Dependent Behaviors in Cardiac Muscle. Phys. Rev. Lett. **82**, 2995 (1999).
- [9] W. Singer. Striving for coherence. Nature, **397** 391, 1999.
- [10] Dutta, S., Parihar, A., Khanna, A. et al. Programmable coupled oscillators for synchronized locomotion. Nat Commun **10**, 3299 (2019).
- [11] P. Bak. The Devil's Staircase. Physics Today **39**, 12, 38 (1986).
- [12] J. A. Lissajous. "Mmoire sur l'Etude optique des mouvements vibratoires," Annales de chimie et de physique, 3rd series, 51 (1857) 147-232
- [13] E. Y. C. Tong, Lissajous figures The Physics Teacher **35**, 491 (1997).
- [14] B. D. Josephson, Phys. Letters **16**, 25 (1962).
- [15] B. D. Josephson, Advan. Phys. **14**, 419 (1965).
- [16] W. C. Stewart CURRENT-VOLTAGE CHARACTERISTICS OF JOSEPHSON JUNCTIONS Appl. Phys. Lett. **12**, 277 (1968).
- [17] S. Shapiro, Josephson currents in superconducting tunneling: the effect of microwaves and other observations, Phys. Rev. Lett. **11**, 80 (1963).
- [18] A. A. Golubov, M. Yu. Kupriyanov, and E. Il'ichev. The current-phase relation in Josephson junctions, Rev. Mod. Phys. **76**, 411 (2004).
quote: Phase engineering techniques are used to control the dynamics of long-bosonic Josephson-junction arrays built by linearly coupling Bose-Einstein condensates.
- [19] Dengling Zhang, Haibo Qiu, and Antonio Muoz Mateo, Unlocked-relative-phase states in arrays of Bose-Einstein condensates, Phys. Rev. A **101**, 063623 (2020).
- [20] M. P. N. Juniper, A. V. Straube, R. Besseling, D. G. A. L. Aarts, and R. P. A. Dullens, Microscopic dynamics of synchronization in driven colloids. Nat. Commun. **6**, 7187 (2015).
- [21] S. Herrera-Velarde and R. Castaeda-Priego, Superparamagnetic colloids confined in narrow corrugated substrates, PHYSICAL REVIEW E **77**, 041407 (2008).
- [22] S. Herrera-Velarde and R. Castaeda-Priego, J. Phys.: Condens. Matter **19**, 226215 (2007).
- [23] C. Lutz, M. Kollmann, and C. Bechinger, Phys. Rev. Lett. **93**, 026001 (2004); C. Lutz, M. Kollmann, C. Bechinger, and P. Leiderer, J. Phys.: Condens. Matter **16**, S4075 (2004).
- [24] See Figure1.mp4 in appropriate